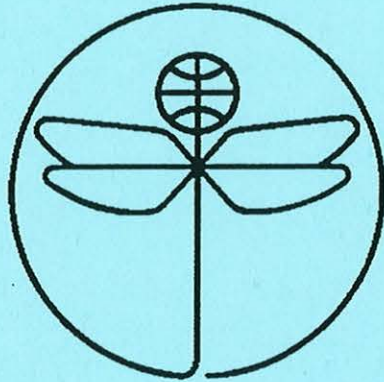


TWENTY FIRST EUROPEAN ROTORCRAFT FORUM



Paper No VII. 3

**THE USE OF INDIVIDUAL CHANNEL ANALYSIS AND DESIGN  
TO MEET HELICOPTER HANDLING QUALITIES REQUIREMENTS**

**BY**

Graham J.W.Dudgeon, Jeremi J. Gribble, John O'Reilly

University of Glasgow  
Glasgow, Scotland

August 30 - September 1, 1995  
SAINT - PETERSBURG, RUSSIA

Paper nr.: VII.3



The Use of Individual Channel Analysis and Design to Meet Helicopter  
Handling Qualities Requirements.

**G.J.W. Dudgeon; J.J. Gribble; J. O'Reilly**

**TWENTY FIRST EUROPEAN ROTORCRAFT FORUM**

August 30 - September 1, 1995 Saint-Petersburg, Russia

# The Use of Individual Channel Analysis and Design to Meet Helicopter Handling Qualities Requirements

Graham J.W. Dudgeon

Jeremy J. Gribble

John O'Reilly

University of Glasgow, Glasgow, Scotland

## Abstract

A control law was designed for a linearised model of a typical combat rotorcraft trimmed to 30 knots forward flight. Although based on a single flight condition, the same controller is found, in simulation, to give level 1 performance for the range of speeds from hover to 80 knots, for handling qualities based on small amplitude motions. Control synthesis was performed using the method of *Individual Channel Analysis and Design* (ICAD). ICAD is a neo-classical, frequency domain control analysis and design method for multivariable systems. Its most distinctive feature is the use of the so-called *multivariable structure functions* which make explicit the role of cross-coupling and quantify its effects on robustness. The control law so obtained is very simple, and the results suggest that modern control methods, based on optimal synthesis, are not a necessity for the helicopter flight control problem.

## Notation

$\beta_{1s}$	Main rotor long. cyclic flapping angle (rad)
$\beta_{1c}$	Main rotor lat. cyclic flapping angle (rad)
$\beta_{10}$	Main rotor coning angle (rad)
$D$	m by m decoupling matrix
$G$	m by m system transfer function matrix
$\gamma$	Multivariable structure function
$\Gamma$	Plant structure function
$K$	m by m diagonal controller matrix
$p, q, r$	Body axes angular velocity components (rad/s)
$S$	m by m shaping filter
$\theta_0$	Main rotor collective
$\theta_{1s}$	Longitudinal cyclic
$\theta_{1c}$	Lateral cyclic
$\theta_{0T}$	Tail rotor collective
$\theta_{0act}$	Main rotor collective actuator state
$\theta_{1sact}$	Longitudinal cyclic actuator state
$\theta_{1cact}$	Lateral cyclic actuator state
$\theta_{0Tact}$	Tail rotor collective actuator state
$\theta, \phi, \psi$	Euler angles (rad)
$u, v, w$	Body axes velocity components (ft/s)
$x$	19th order state vector
$x_{rigidbody}$	Rigid body state vector
$x_{rotor}$	Main rotor state vector
$x_{actuator}$	Actuator state vector

## Introduction

The publication in 1988 of the revised helicopter handling qualities requirements ADS-33C [1] has provided a focus for much research into the helicopter flight control problem, by both academic and industrial workers. The highly coupled nature of rotorcraft dynamics has been thought to preclude the use of 'one-loop-at-a-time' control design methods, based on classical single-input-single-output (SISO) techniques. Hence, much of the research published in the last few years has concentrated on the use of Modern Control Techniques such as eigenstructure assignment [2],  $H_\infty$  optimal synthesis [3] and Linear Quadratic Gaussian optimal synthesis with Loop Transfer Recovery [4]. Methods such as these have the advantage that they can be used to compute all the SISO elements of a multiloop controller at once. Furthermore, if robustness is assessed within the singular value framework, then statements can be made about the stability robustness of the resulting designs with respect to plant model error. On the other hand, many of the advantages of the classical approach are lost. For example, it is relatively difficult to relate the weighting functions that constitute the design parameters of the various optimal control methods to system performance in a transparent way. Singular values, that are often used to assess system performance and robustness, are abstract mathematical concepts that may be difficult to interpret physically. Finally, the resulting control laws are usually of relatively high order in contrast to classically designed controllers (for SISO plants) which are no more complicated than they need to be in order to meet the specifications.

This paper is concerned with the application of *Individual Channel Analysis and Design* ([5] and [6]) to a model of a typical single main rotor combat helicopter [7] in order to obtain multivariable control laws that meet the specifications contained within ADS-33C. Individual Channel Analysis and Design (ICAD) is a frequency domain based framework for the analysis and design of multivariable control laws. Its main feature is the use of the so-called *multivariable structure functions* to characterise the coupling between the input-output pairs ('channels') of the plant. The structure functions quantify whether the loop interaction is small or large and, if



large, whether it is benign or malign. They can be used to generate effective channel transfer functions upon which the design of individual diagonal elements of the feedback control law can proceed using classical techniques of the Nyquist-Bode type. Finally, the structure functions are used to supplement the channel stability margins, obtained by breaking one loop at a time, to provide a framework for analysing stability robustness in a transparent way that takes into account the effects of loop interaction. Since the synthesis of individual diagonal elements of the feedback control matrix is performed using classical SISO techniques, these elements are of relatively low order and are no more complicated than necessary, making controllers of this type eminently suitable for gain-scheduling.

Previous studies of the helicopter flight control problem using the ICAD method [8] have concentrated on analytical issues and have addressed the problem of designing for good handling qualities in only a preliminary fashion. Furthermore, this earlier work was hampered by an inappropriate choice of plant outputs. A detailed examination of the specifications clarifies which outputs should be used, and makes the design problem very much easier.

In the following sections of the paper a brief description of the ICAD method is presented. The relevant performance specifications from [1] are then summarised and the implications of the structural properties of the plant, as revealed by individual channel *analysis*, for *design* to meet those specifications are discussed. The bulk of the paper is taken up with presenting, assessing and discussing the predicted handling qualities of a particular ICAD based design. The authors expect the conference presentation to include the results from non-linear simulations.

### Outline of Individual Channel Analysis and Design

This section describes the control analysis and design methodology that was used, and includes a brief outline of the Individual Channel Analysis and Design (ICAD) approach to the level needed to understand the paper. The reader should consult [5,6] for a more detailed description.

The aircraft is modelled as an  $m$ -by- $m$  transfer function matrix  $G$ . A diagonal control matrix  $K$  is in the forward path, immediately before  $G$ , and a feedback loop is closed around  $GK$ . In ICAD attention is focused on the transfer functions obtained by opening some of the loops while leaving the remainder closed. For this brief review it is appropriate to concentrate on the case where the loops are opened one at a time. Without loss of

generality, suppose that loop 1 is opened between output 1 of the plant and the input, to the (1,1) element of the diagonal controller  $K$ . (This can always be done by renumbering the plant input-output pairs.) Let  $G$  be partitioned as

$$G = \begin{bmatrix} g_{11} & g_{12} \\ g_{21} & g_{22} \end{bmatrix} \quad (1)$$

where  $g_{11}$  is a scalar,  $g_{12}$  is a 1-by- $(m-1)$  row vector,  $g_{21}$  is a  $(m-1)$ -by-1 column vector and  $g_{22}$  is a  $(m-1)$ -by- $(m-1)$  matrix. (All other matrices and vectors are also appropriately partitioned.) A block diagram of the configuration is given in figure 1. The plant output  $y_1$  is given by:

$$y_1 = C_1 e_1 + L_1 y_2^{\text{ref}} \quad (2)$$

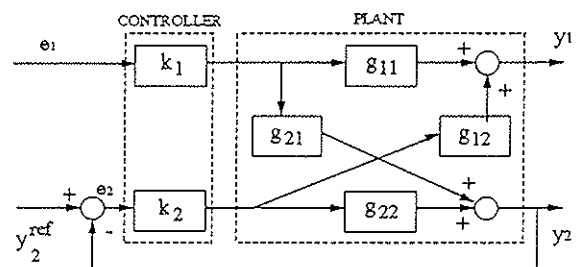


Figure 1. Block Diagram of ICAD configuration.

where  $e_1$  is the input to the (1,1) element  $k_1$  of diagonal controller  $K$ , and  $y_2^{\text{ref}}$  is the  $(m-1)$ -by-1 column vector of reference values for the outputs other than the first. Define:

$$\begin{aligned} C_1 &= (g_{11} - g_{12} h_2 g_{22}^{-1} g_{21}) k_1 & (a) \\ L_1 &= g_{12} h_2 g_{22}^{-1} & (b) \\ h_2 &= (I_2 + k_2 g_{22})^{-1} k_2 g_{22} & (c) \end{aligned} \quad (3)$$

SISO transfer functions such as  $C_1$  play an important part in ICAD, and are called *channels*. The frequency response of channel  $C_1$  can be used to analyse the transient response and reference tracking of  $y_1$  for the *nominal* system in exactly the same way as in a classical, single loop system. The MISO transfer function  $L_1$  from  $y_2^{\text{ref}}$  to  $y_1$ , which does not depend on  $k_1$  represents the effects of changes in reference signal in channels other than the first and shows that these can be regarded as external disturbances to channel 1, whose disturbance rejection properties are also quantified by  $C_1$ .

All of the foregoing is well known. The contribution of ICAD is to recognise that the form of (3a) has implications for the sensitivity of  $C_1$  with respect to variations in the plant model, and hence also for

performance and stability robustness; particularly the latter. Equation (3a) shows that  $C_1$  is the sum of two contributions. The first contribution goes directly from plant input 1 to output 1 via  $g_{11}$ , the other contribution goes through the rest of the plant, and the associated controllers. Defining

$$\hat{g}_{11} \equiv -g_{12}h_2g_{22}^{-1}g_{21} \quad (4)$$

$C_1$  can be expressed as  $C_1 = (g_{11} + \hat{g}_{11})k_1$ . Note that  $\hat{g}_{11}$  does not depend on  $g_{11}$ . The stability robustness of channel 1 after loop closure with respect to variations in  $G$  is now examined. The return difference,  $R_1$ , associated with channel 1 is given by

$$R_1 \equiv I + C_1 \quad (5)$$

and the relative error,  $\Delta R_1/R_1$ , in  $R_1$  is then given by

$$\frac{\Delta R_1}{R_1} = \frac{C_1}{I + C_1} \left( \frac{I}{I - \gamma_1} \frac{\Delta g_{11}}{g_{11}} + \frac{-\gamma_1}{I - \gamma_1} \frac{\Delta \hat{g}_{11}}{\hat{g}_{11}} \right) \quad (6)$$

where the multivariable structure function  $\gamma_1$  is defined by

$$\gamma_1 \equiv -\frac{\hat{g}_{11}}{g_{11}} = g_{11}^{-1}g_{12}h_2g_{22}^{-1}g_{21} \quad (7)$$

Note that all errors in the remainder of the plant apart from  $g_{11}$  are lumped into  $\Delta \hat{g}_{11}$ . Channel 1 may be regarded as possessing stability robustness if the factors multiplying  $\Delta g_{11}/g_{11}$  and  $\Delta \hat{g}_{11}/\hat{g}_{11}$  on the right hand side of (6) are not too large. Following classical control practice this requires that the frequency responses of  $C_1$  and  $-\gamma_1$  both have good gain and phase margins with respect to the -1 point on their polar plots, and good behaviour between the two cross-over frequencies. (In practice, one usually plots  $+\gamma_1$  and measures margins from the +1 point.) The overall system is regarded as robust if these conditions are satisfied for all channels. What is new in ICAD, that would not be apparent from considering  $C_1$  and the other channels by themselves, is that robustness problems are likely to arise if the frequency responses of any of the structure functions pass close to +1 at frequencies lower than (say) the -180° crossovers of their associated channels. (Reference [6] provides general formulae for the multivariable structure functions. Alternatively, the formulae of this section can be used if the channels are temporarily renumbered.)

These concepts and formulae can be used directly to assess the performance and stability robustness if all of the elements of the controller are known or, at a pinch, to design the final element if the other  $m-1$  are known. In practice, the designer starts from a point where none of the controller's elements are known. Progress can be made by making appropriate approximations, the simplest scheme being the *constrained variable method* [9]. In this method, it is assumed that  $k_1$  (for example) can be designed assuming that all of the other feedback loops are infinitely tight in the sense that  $h_2 \approx I_2$ . This forms the approximate channel function

$$\begin{aligned} \tilde{C}_1 &= g_{11}(I - \Gamma_1)k_1 \\ \Gamma_1 &= g_{11}^{-1}g_{12}g_{22}^{-1}g_{21} \approx \gamma_1 \end{aligned} \quad (8)$$

The *plant structure functions*  $\Gamma_i$  ( $i=1-m$ ) depend on the  $G$ , but not on  $K$ . They may be regarded as measures of the conditioning of the matrix  $G$  and can be used to assess the potential for robustness problems before the design process starts. For example, from working similar to that leading to equation (6), it can be shown that the approximate channel transfer functions used in the constrained variable method will be extremely sensitive to plant model error at frequencies where the polar plot of  $\Gamma_1$  goes close to +1.

A final important result can be derived from Schur's formula for the determinant of a partitioned matrix, namely

$$|G| = g_{11}|g_{22}||I - \Gamma_1| \quad (9)$$

The plant's *transmission zeros* may be defined as those values of  $s$  where  $|G(s)| = 0$ . Equation (9) indicates that if the frequency response of  $\Gamma_1$  goes close to +1 at some frequency it may be because the plant model has transmission zeros in the vicinity of the imaginary axis. Equivalently, if the plant model has transmission zeros close to the imaginary axis, it is likely that there will be robustness problems at frequencies similar to the absolute values of the zeros.

The number of right hand plane poles and zeros (RHPPs and RHPZs) of an open-loop transfer function plays an important role in ICAD theory, and is referred to as the *structure*. The number of RHPZs of a channel can be computed by counting the number of encirclements of the (+1,0) point of the frequency response of the appropriate multivariable structure function. The number of right hand plane transmission zeros of the plant model is related to the plant structure functions in a similar way [6].

## Handling Qualities

Handling Qualities (HQ) Specifications as stated in ADS-33C [1] are categorised in terms of response types from which flying qualities 'levels' can be assessed. The response types are dependent on specific mission task elements (MTEs) such as target acquisition and tracking, which requires attitude command attitude hold (ACAH) response. Other response types include rate command direction hold (RCDH) which is necessary for a MTE which requires a fixed flight path such as slope landing, and translational rate command (TRC) which is necessary for a precision hover task.

Flying qualities 'levels' are derived from the Cooper-Harper pilot ratings scale and are defined in table 1.

**Table 1. Definition of 'Levels'.**

Level 1	MTE can be completed with minimal pilot compensation. - Satisfactory without improvement.
Level 2	MTE can be completed but requires moderate/considerable pilot compensation. - Deficiencies warrant improvement
Level 3	Considerable pilot workload needed to maintain control of rotorcraft. - Deficiencies require improvement

The HQ specifications to meet a required level are defined in both the time domain and the frequency domain when considering small amplitude signals. The frequency domain specifications relate to the response the pilot 'sees' (i.e. the closed loop augmented system) and ensures the pilot feels a sufficient bandwidth (BW) and acceptable phase delay between commanded response and actual response. Two bandwidths must be considered, the phase limited bandwidth and the gain limited bandwidth. Figure 2 shows the definition of the two bandwidths and the phase delay parameters.

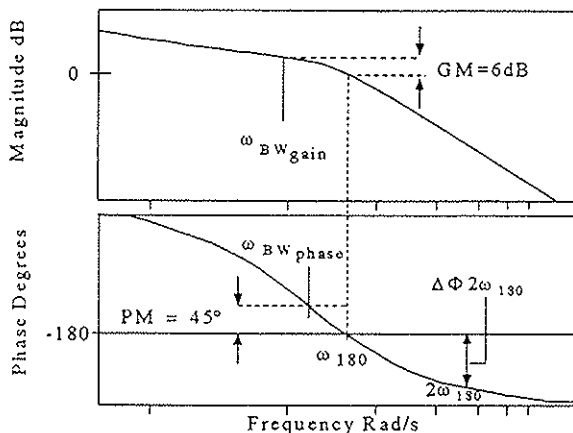


**Figure 2. Definitions of BWs and phase delay.**

The phase delay is calculated as,

$$\tau_p = \frac{\Delta\phi 2\omega_{180}}{57.3(2\omega_{180})} \quad (10)$$

For ACAH, the specifications state that the pilot must have at least 6dB of gain margin to reduce the possibility of pilot-induced oscillations (PIOs) when manoeuvring aggressively. This requires that  $\omega_{BW_{phase}}$  is less than  $\omega_{BW_{gain}}$ . The HQ bandwidth,  $\omega_{BW}$ , is taken to be the lesser of  $\omega_{BW_{phase}}$  and  $\omega_{BW_{gain}}$ , except for ACAH response types where  $\omega_{BW} = \omega_{BW_{phase}}$ . The time domain requirements specify bounds on cross coupling, damping and in the case of height rate, the shape of response. Level 1 is clearly the level which should be aimed for when designing a control system.

## Handling Qualities Outputs

The outputs of the helicopter which are to be controlled must be determined. These outputs should be easily related to the HQ specifications. To aid the decision for which outputs to choose, table 2 shows a list of the small signal specifications for hover and low speed, which are the appropriate specifications for a linear design at 30 knots. Also shown in table 2 is the related output(s) for the specification and whether the assessment is done in the time or the frequency domain.

From table 2 it is seen  $\dot{h}$ ,  $\theta$ ,  $\phi$  and  $\psi$  or  $r$  are natural choices for the controlled outputs. For the purpose of yaw damping, the yaw rate  $r$  will be controlled instead of  $\psi$ . The HQ bandwidth assessment must still be done on  $\psi$ , however.  $\dot{h}$ ,  $\theta$ ,  $\phi$  and  $r$  will be controlled by  $\theta_0$ ,  $\theta_{1s}$ ,  $\theta_{1c}$  and  $\theta_{0T}$  respectively. It is beneficial to also feed back pitch-rate  $q$  with  $\theta$  and roll-rate  $p$  with  $\phi$  to aid pitch and roll damping.

In straight and level flight,

$$q \equiv \dot{\theta} \quad (11)$$

$$p \equiv \dot{\phi} \quad (12)$$

and so by adding a multiple  $k$  of the rate signal to the attitude signal (e.g.  $\theta + kq$ ) a zero is effectively introduced into the attitude channel at a frequency of  $k^{-1}$  rad/s. This means a substantial phase margin is easier to obtain in the design process due to the phase lead of the apparent zero. For the longitudinal cyclic,  $\theta + q$  was chosen for feedback and for the lateral cyclic  $\phi + 0.1p$  was chosen. The values of  $q$  and  $p$  were chosen using classical loop shaping considerations.

**Table 2. ADS-33C small signal requirements for hover and low speed**

Section	Page	Title	Output(s)	Domain
3.3.2	17	Small Amplitude Pitch (Roll) Attitude Changes	$\theta, \phi$	Frequency, Time
3.3.5	23	Small Amplitude Yaw Attitude Changes	$\psi$	Frequency, Time
3.3.9	26	Interaxis Coupling	$\dot{h}, \theta, \phi, r$	Time
3.3.9.1	26	Yaw due to Collective	$\dot{h}, r$	Time
3.3.9.2	27	Pitch to Roll (Roll to Pitch)	$\theta, \phi$	Time
3.3.10	27	Response to Collective	$\dot{h}$	Time
3.3.10.1	27	Height Response Characteristics	$\dot{h}$	Time

**Individual Channel Analysis (ICA) of the Helicopter Model**

The purpose of ICA [5,6] is to determine whether the presence (and location within the model) of RHPPs and RHPZs, i.e. the structure, will introduce problems both in terms of the design procedure and stability robustness. Any such problems can be resolved within the ICA framework and the use of Individual Channel Design (ICD) [5,6] can proceed straightforwardly.

The analysis and design is based on a 19th order representation of a typical combat rotorcraft in straight and level flight at 30 knots. The model has 9 rigid body states, 6 rotor states and 4 actuator states (see Appendix). 30 knots was chosen as it is the midpoint of the low speed range. To analyse the  $\Gamma$ 's it was necessary to use the 9th order rigid body model as it was found that computational difficulties arise if the 19th order model is used, thus causing loss of confidence in the structural assessment. Because the higher order dynamics are stable the structure of the 19th order  $\Gamma$ 's will be the same as the 9th order ones. As the design will proceed on the 19th order model it would be beneficial to assess if it is valid to include the 9th order  $\Gamma$ 's in the 19th order formulation. Figure 3 shows the bode plots of the 9th order and the 19th order  $\Gamma_2$ , which relates to the pitch channel.

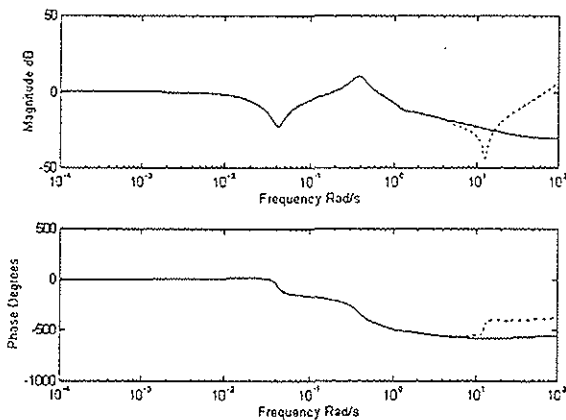


**Figure 3. 9th order and 19th order (---)  $\Gamma_2$**

It is seen that they are similar up to 5 rad/s, as with the other  $\Gamma$ 's. As this will be higher than any channel bandwidths then it is valid to use the lower order  $\Gamma$ 's. The 19th order  $g_{ii}$ s must still be used as they include higher order effects which show themselves below 5 rad/s.

An alternative mathematical representation of  $\Gamma_i$  and  $\gamma_i$  is now given, which offers more visibility to the structural issues, for a plant which has more than 2 inputs and 2 outputs, than the representation given in equations (7) and (8).

$\Gamma_i$  of a square m by m system can be written as [6],

$$\Gamma_i = \frac{-|G_i|}{g_{ii}|G^i|} \quad i=1\dots m \quad (13)$$

where  $G_i$  is the matrix obtained from  $G$  by setting element (i,i) to zero, and  $G^i$  is the matrix obtained from  $G$  by eliminating the ith row and the ith column.  $g_{ii}$  is element (i,i) of  $G$ .

$\gamma_i$  of a square m by m system can be written as [6],

$$\gamma_i = \frac{-|\bar{G}_i|}{g_{ii}|\bar{G}^i|} \quad i=1\dots m \quad (14)$$

where  $\bar{G}$  varies from  $G$  only in its diagonal elements which instead of  $g_{jj}$  ( $j=1\dots m$ ) are defined as  $k_j^{-1} + g_{jj}$ , where  $k_j$  is the controller of the jth channel.

As an illustration  $\Gamma_1$  and  $\gamma_1$  for a 4 by 4 system will now be shown and they will also be useful to illustrate the structural issues to be discussed.

$$\Gamma_1 = \frac{\begin{vmatrix} 0 & g_{12} & g_{13} & g_{14} \\ g_{21} & g_{22} & g_{23} & g_{24} \\ g_{31} & g_{32} & g_{33} & g_{34} \\ g_{41} & g_{42} & g_{43} & g_{44} \end{vmatrix}}{\begin{vmatrix} g_{22} & g_{23} & g_{24} \\ g_{32} & g_{33} & g_{34} \\ g_{42} & g_{43} & g_{44} \end{vmatrix}} \quad (15)$$

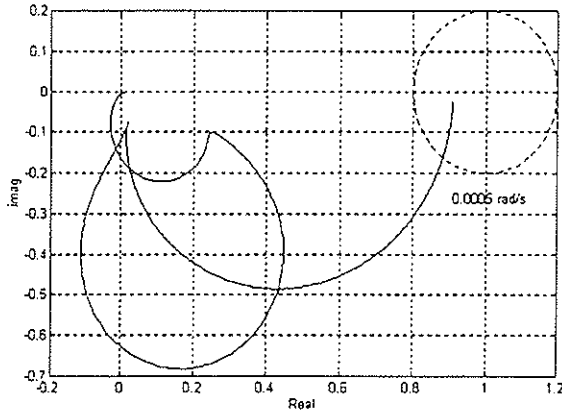


Figure 4. Nyquist plot of  $\Gamma_1$

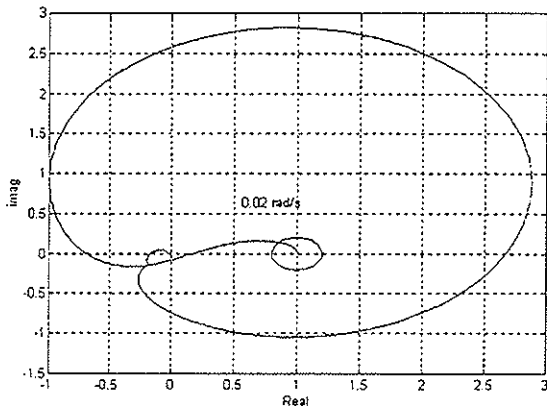


Figure 5. Nyquist plot of  $\Gamma_2$

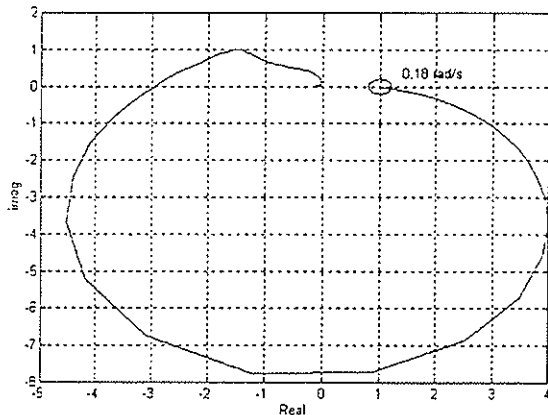


Figure 6. Nyquist plot of  $\Gamma_3$

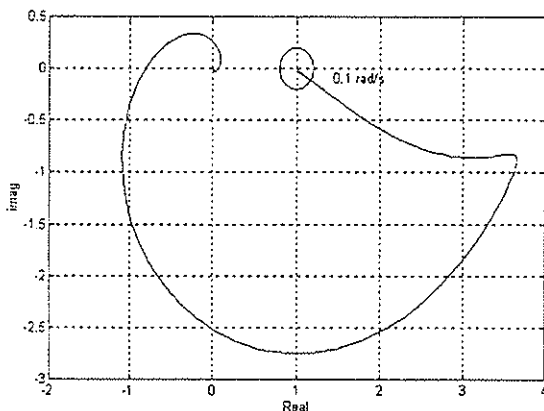


Figure 7. Nyquist plot of  $\Gamma_4$

It can be seen that at low frequencies plant uncertainty could cause one or more of the  $\Gamma$ 's to traverse the  $(+1,0)$  point and hence cause a RHPZ to be introduced into the system, causing a potential stability problem. The proximity of the  $\Gamma$ 's to the  $(+1,0)$  point at low frequency is an interesting effect which has been observed with many helicopter models in forward flight when analysed using ICA. There are two questions to be asked. What can be done to alleviate the problem? Is this sensitivity actually a problem in the context of helicopter control?

To alleviate the problem one must ensure that there is insufficient gain at the problematic frequencies to cause stable poles to move across to the RHP, i.e. the system should be made stability robust. This is done by effectively opening the loops at low frequencies. This approach, however, is fraught with problems as there will be little or no performance robustness (time response invariance in the presence of plant variations) due to the lack of tight feedback control at low frequencies. One must trade off, as always, performance robustness and stability robustness.

Because the high sensitivity region is at such low frequencies it may not be necessary to attempt a control strategy to alleviate the problem. The reason for this is as follows: Any RHPPs which may arise due to low frequency RHPZs will themselves be at low frequencies. ADS-33C [1] does not state that a helicopter has to be absolutely stable, and as the time domain requirements do not specify consideration of responses after 12 seconds then it seems that as long as any unstable mode does not show itself for the first 12 seconds of a response then level 1 handling qualities can still be met. Another argument in favour of regarding the low-frequency sensitivity as non-problematic is that the pilot will be more than capable of controlling such a slow instability with minimal workload.

With these two points in mind it was decided not to open the loops at low frequencies.

### Design Considerations

With the structural issues resolved the design can now proceed. A set of specifications must be determined for the design. ADS-33C [1] states that the height rate response should have a qualitative first order appearance defined by the following transfer function,

$$\frac{\dot{h}}{\theta_0} = \frac{K \exp(-\tau_{\text{bcq}} s)}{T_{\text{bcq}} s + 1} \quad (19)$$



where, for level 1,  $\tau_{\text{bec}}$  is no greater than 0.2 secs and  $T_{\text{bec}}$  is no greater than 5 secs [1].  $K$  in eqn (19) is a gain factor. This specification should not be difficult to obtain if one aims for a smooth 0dB crossover of approximately 1 rad/s and a phase margin of at least 60 degrees. Because of the slow rise time it is possible to reduce the bandwidth even further but this will cause increased height rate cross coupling when the other channels are excited. The height rate response must be 'fitted' to eqn (19) and have a coefficient of determination of between 0.97 and 1.03 [1]. The damping of the  $\theta$ ,  $\phi$  and  $\psi$  responses to pulse inputs at the appropriate inceptor should be at least 0.35, this is expected to be met if all 0dB crossover regions are smooth and the phase margins are adequate.

The handling qualities bandwidth specifications relate to the pitch, roll and yaw rate channels. As mentioned previously, for ACAH the phase limited bandwidth must be less than the gain limited bandwidth to ensure the pilot has a gain margin of 6dB for aggressive manoeuvring. For this design ACAH is the response type of the pitch and roll channel. Table 6 shows bandwidth and phase delay specifications which will meet level 1 for target acquisition and tracking, the most stringent requirement..

Table 6. Handling Qualities BW to meet level 1.

Response	BW	Phase/Gain Lim.	phase delay
$\theta$	>2	phase	<0.16
$\phi$	>3.5	phase	<0.16
$\psi$	>3.5	-	<0.16

The phase delay is expected to be within level 1 bounds because the phase does not drop sufficiently at high frequency to cause problems. To meet the HQ bandwidth requirements it is necessary to consider three things in the open loop design. These are,

1. The 0dB crossover frequency
2. The phase margin
3. The 180° crossover frequency

Knowing 1. and 2. it is known what the closed loop phase will be at the 0dB frequency,  $\omega_{0dB}$ , and by 3. it is known that the closed loop 180° frequency,  $\omega_{180}$ , is at the same frequency as the open loop. With this knowledge one can assess approximately where the phase limited bandwidth is situated by assuming that the phase decrease between  $\omega_{0dB}$  and  $\omega_{180}$  in the closed loop is linear on the logarithmic scale. To ensure that the phase limited bandwidth is less than the gain limited bandwidth a gain margin of at least 12 dB should be allowed for (It must be remembered that the ACAH bandwidth assessments are performed on  $\theta$  and  $\phi$  and not  $\theta+q$  and  $\phi+0.1p$ ). The

open loop requirements for the latter should be set correspondingly higher to compensate for the fact that the closed loop  $\theta$  and  $\phi$  channels have poles effectively situated at 1 rad/s and 10 rad/s respectively, relative to  $\theta+q$  and  $\phi+0.1p$ . The open loop specifications can now be stated and are shown in table 7. The cross shown for the 180° crossover for the height rate channel indicates that the crossover can be placed arbitrarily, as there is no bandwidth requirement on the height rate response. However, an adequate gain and phase margin is required, as with all the channels, for stability robustness. These specifications are approximate and are not lower bounds which must be strictly met.

Table 7. Open loop specifications

Channel	0dB crossover rad/s	180° crossover rad/s	PM degs	GM dB
$h$	1	x	60	10
$\theta+q$	3	10	50	12
$\phi+0.1p$	3	10	50	12
$r$	5	25	50	20

The predicted HQ bandwidths calculated from the open loop specifications are shown in table 8 and are seen to be level 1.

Table 8. Predicted handling qualities BWs

Response	Predicted HQ BW rad/s
$\theta$	2.6
$\phi$	3.9
$\psi$	3.7

### Individual Channel Design (ICD)

The first channel must be designed on the basis that the other three channels are tightly closed. To ensure that this is a valid approximation the channel with the lowest bandwidth should be chosen as the first. The reason for this is that at the crossover frequency the other channels, when they have been designed, will essentially be tight due to their higher bandwidths, and so the constrained channel will be a very good approximation to the actual channel. Once the height rate controller has been designed its effects will be included in the design of the next channel and so element (1,1) of  $G^i$  and  $G_i$  of eqn. (13) will be replaced by  $k_i^{-1} + g_{11}$ . As the yaw rate channel has the largest crossover frequency, it will be designed last. The bandwidth separation principle cannot be applied to the pitch and roll channels as they are to be designed to have similar crossovers. A way to ease this problem is to numerically calculate what the gain and phase of the controllers must be for the channels at the desired crossover frequency. By ensuring the controllers are set to have this gain and phase at that frequency then the need to perform

$$\gamma_1 = \begin{array}{c} \left| \begin{array}{cccc} 0 & g_{12} & g_{13} & g_{14} \\ g_{21} & k_2^{-1} + g_{22} & g_{23} & g_{24} \\ g_{31} & g_{32} & k_3^{-1} + g_{33} & g_{34} \\ g_{41} & g_{42} & g_{43} & k_4^{-1} + g_{44} \end{array} \right| \\ \left| \begin{array}{cccc} k_2^{-1} + g_{22} & g_{23} & g_{24} & \\ g_{11} & g_{32} & k_3^{-1} + g_{33} & g_{34} \\ & g_{42} & g_{43} & k_4^{-1} + g_{44} \end{array} \right| \end{array} \quad (16)$$

Consider element  $(j,j)$  ( $j=2..4$ ) of the numerator of eqn. (15), which can be rewritten in two equivalent forms,

$$k_j^{-1} + g_{jj} = \frac{g_{jj}}{h_j} \quad (a)$$

$$= \frac{1}{k_j} (1 + k_j g_{jj}) \quad (b) \quad (17)$$

where  $h_j$  is the single-loop subsystem  $k_j g_{jj} / (1 + k_j g_{jj})$ .

From 17(b) it is obvious that the number of RHPZs of  $k_j^{-1} + g_{jj}$  is dependent on the number of encirclements of the  $(-1,0)$  point of  $k_j g_{jj}$ , and hence the structure of  $\gamma_1$  is dependent on each  $k_j g_{jj}$  ( $j=1..m$ ,  $j \neq i$ ). This is an important result and suggests that to design successfully not only must the structure of the individual channels of the system be considered, but also the structure of the individual transfer functions  $g_{jj}$ .

### Channel Structural Analysis

To analyse the structure of the helicopter it is necessary to initially consider each open loop channel with the approximation that the other three channels are tightly closed. i.e. they have infinite gain control. These approximate channels shall be referred to as constrained channels.

The  $i$ th constrained channel is,

$$\tilde{C}_i = g_{ii}(1 - \Gamma_i) \quad (18) \\ i=1..m$$

The number of RHPPs and RHPZs of eqn.(18) is known and by inspecting the Nyquist plot of  $\tilde{C}_i$  it can be established whether the channel can be stabilised by the introduction of a controller with feedback. The four channels are investigated in this way and if all four channels can be stabilised, then the structure of each  $\Gamma_i$  is correct for stability. Hence the designer should insure that the structure of  $\gamma_1$  is the same as  $\Gamma_i$ . The structure of the four  $\tilde{C}_i$ 's is shown in table 3 with an indication whether closed loop stability is possible practically.

Table 3. Structure of constrained channels

$\tilde{C}$	RHPZs	RHPPs	Can be stabilised?
$g_{11}(1-\Gamma_1)$	None	None	Yes
$g_{22}(1-\Gamma_2)$	None	None	Yes
$g_{33}(1-\Gamma_3)$	None	None	Yes
$g_{44}(1-\Gamma_4)$	None	None	Yes

Table 3 shows that the actual channels should have the same structure as the constrained channels below crossover frequency. To do this it is necessary to make the structure of  $k_j^{-1} + g_{jj}$  the same as  $g_{jj}$  ( $j=1..4$ ). This must be able to be done, however, with the same control strategy that will stabilise the channels.

To illustrate the above discussion, a simple example will now be shown. With a view to stabilise the 19th order model, table 4 shows the most basic control needed to stabilise each constrained channel, whereas table 5 shows the most basic control needed to insure each  $k_j^{-1} + g_{jj}$  is the same structure as  $g_{jj}$ , the basic control action for stability includes unity negative feedback.

Table 4. Control action needed for stability

$\tilde{C}$	Control Action
$g_{11}(1-\Gamma_1)$	Gain
$g_{22}(1-\Gamma_2)$	Gain
$g_{33}(1-\Gamma_3)$	Negative Gain
$g_{44}(1-\Gamma_4)$	Negative Gain

Table 5. Control action needed for structural equivalence

Individual TF	Control Action
$g_{11}$	Gain
$g_{22}$	Gain
$g_{33}$	Negative Gain
$g_{44}$	Negative Gain

From tables 4 and 5 it can be seen that the basic control action is the same to stabilise the constrained channels and to achieve structural equivalence, hence the above control action will stabilise the plant.

### Structural Sensitivity

The analysis is not complete at this stage. The  $\Gamma$ 's must be examined to establish whether plant uncertainty is likely to introduce RHPZs into the system. Figures 4-7 show the  $\Gamma$ 's in Nyquist Form. A non-robust region of radius 0.2 around the  $(+1,0)$  point [8] is also shown with the frequency where the non-robust region is entered.

trial and error iterations of the design is reduced. The numerical calculation is done simply by solving the four channel equations as shown below,

$$\begin{aligned} k_1 g_{11}(1 - \gamma_1) \Big|_{\omega=1} &= 1 \angle 120^\circ \\ k_2 g_{22}(1 - \gamma_2) \Big|_{\omega=3} &= 1 \angle 130^\circ \\ k_3 g_{33}(1 - \gamma_3) \Big|_{\omega=3} &= 1 \angle 130^\circ \\ k_4 g_{44}(1 - \gamma_4) \Big|_{\omega=5} &= 1 \angle 130^\circ \end{aligned} \quad (20)$$

The channel controllers so designed, using classical loop shaping, are given by,

$$k_1(s) = \frac{0.13(s+1)}{s(s+10)} \quad (21)$$

$$k_2(s) = \frac{0.25(s+2)(s+2.1)}{s(s+3.4)(s+25)} \quad (22)$$

$$k_3(s) = \frac{-0.129(s+3.2)(s^2+0.16s+0.15)}{s(s^2+132s+0.69)(s+13)} \quad (23)$$

$$k_4(s) = \frac{-0.72(s+2)}{s(s+25)} \quad (24)$$

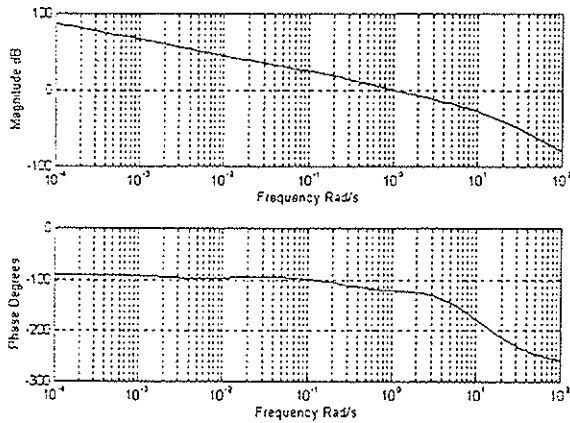


Figure 8. Bode plot of open loop height rate channel

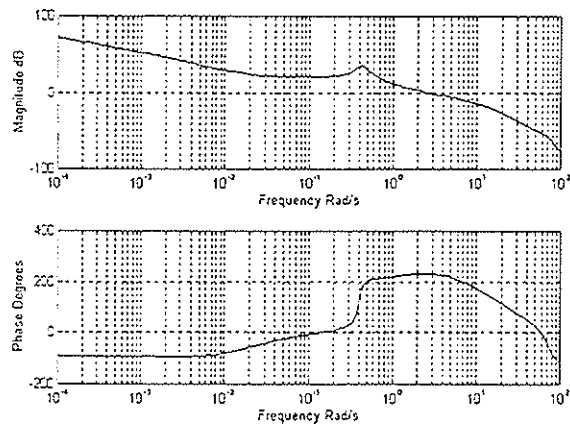


Figure 9. Bode plot of open loop  $\theta+q$  channel

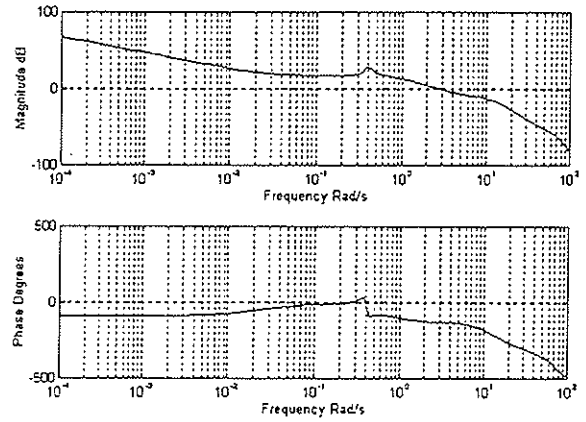


Figure 10. Bode plot of open loop  $\phi+0.1p$  channel

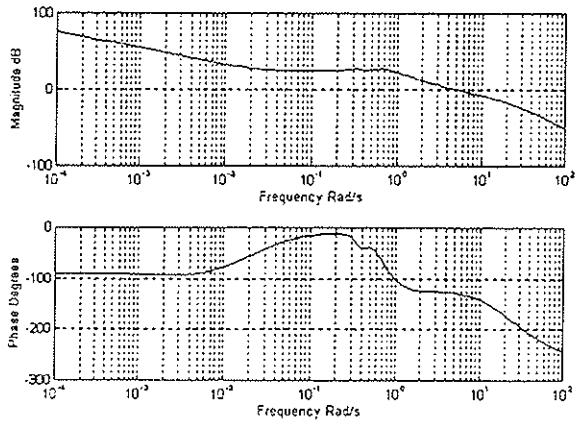


Figure 11. Bode plot of open loop yaw rate channel

The open loop bode plots for each channel is shown in figures 8-11. Table 9 lists the 0dB crossovers, the 180 degrees crossovers and the gain and phase margins. With the controllers in place it was found that the  $\gamma$ 's (the MSFs) were equivalent to the  $\Gamma$ 's (the PSFs) at the frequencies of interest and so the introduction of the diagonal controller did not introduce additional sensitivity problems.

A decoupling element was also needed to reduce the yaw rate due to collective cross coupling, given by,

$$d_{41}(s) = \frac{-5s(s+0.01)(s+0.08)}{(s+0.5)(s+1)^2(s+10)} \quad (25)$$

and a shaping filter was required for the height rate response, given by,

$$f_1(s) = \frac{12(s+1)}{(s+0.6)(s+20)} \quad (26)$$

Table 9. Open loop results

Channel	0dB crossover rad/s	180° crossover rad/s	PM degs	GM dB
$\dot{h}$	1.0	10.0	58.4	28.4
$\theta+q$	2.6	9.5	50.7	13.4
$\phi+0.1p$	2.7	9.8	49.6	12.6
$r$	4.8	23.6	52.2	19.7

The control structure is shown in figure 12.

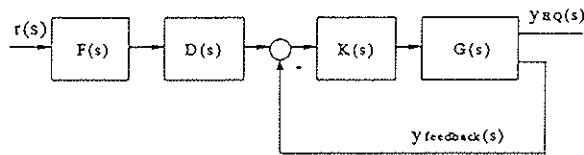


Figure 12. Control Structure

where,

$$F(s) = \text{diag}\{f_1(s), 1, 1, 1\} \quad (27)$$

$$D(s) = \begin{bmatrix} 1 & 0 & 0 & 0 \\ 0 & 1 & 0 & 0 \\ 0 & 0 & 1 & 0 \\ d_{41}(s) & 0 & 0 & 1 \end{bmatrix} \quad (28)$$

$$K(s) = \text{diag}\{k_1(s), k_2(s), k_3(s), k_4(s)\} \quad (29)$$

The step responses for the augmented system at 30 knots are shown in figures 13-16.

Analysing the control law from hover to 80 knots it was found that level 1 handling qualities for all the criteria considered in table 2 were met. The results are shown in figures 17-20. Roll to pitch and pitch to roll cross coupling remained under the required value of 25% for level 1. Damping of the  $\theta$ ,  $\phi$  and  $\psi$  responses remained greater than 0.35. It should be noted that the forward flight requirements are equivalent to the hover and low speed requirements considered here.

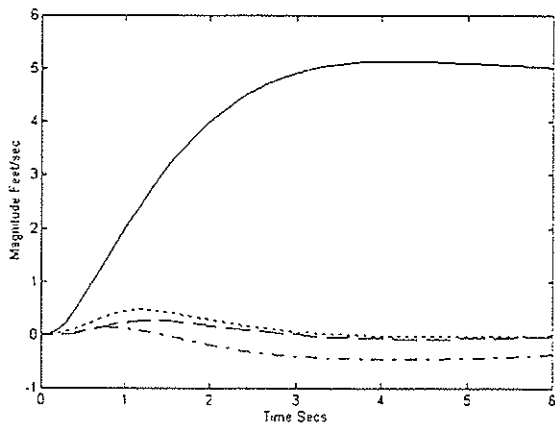


Figure 13. Height rate step response

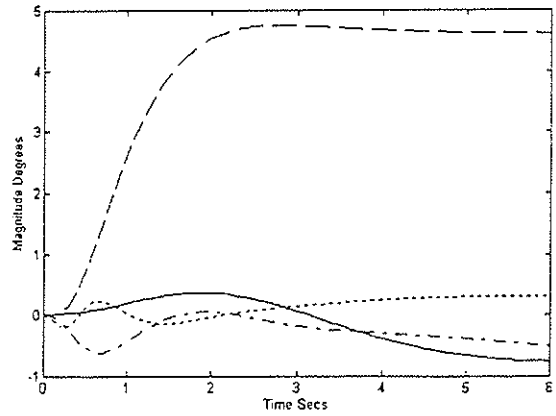


Figure 14. Pitch attitude step response

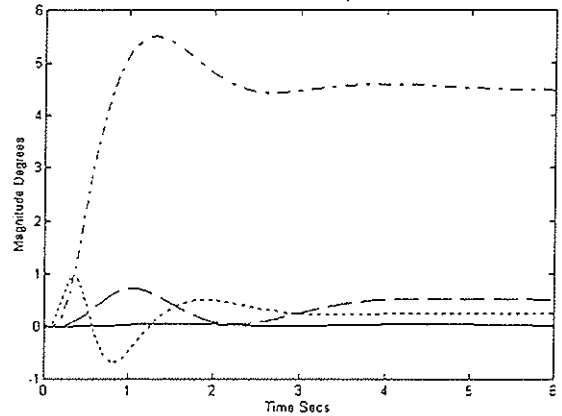


Figure 15. Roll attitude step response

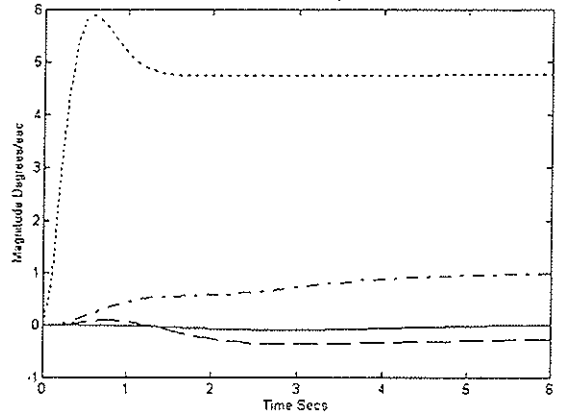


Figure 16. Yaw rate step response

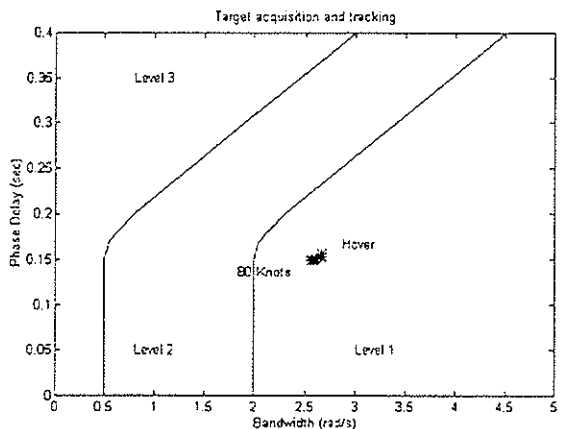


Figure 17. Pitch attitude HQ BW and phase delay

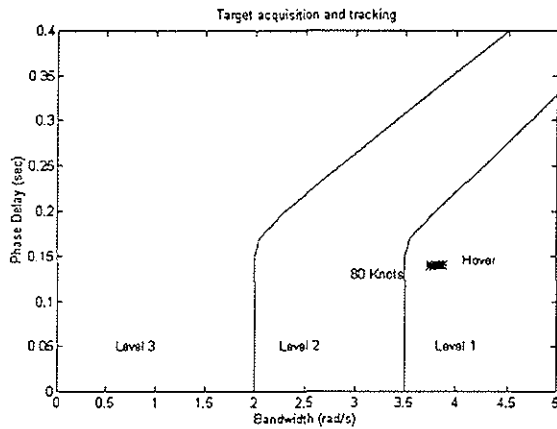


Figure 18. Roll attitude HQ BW and phase delay

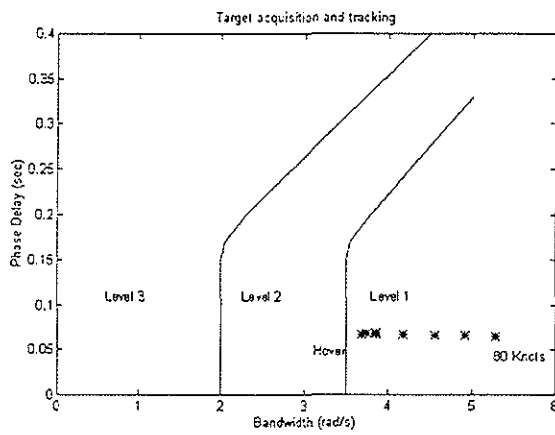


Figure 19. Yaw attitude HQ BW and phase delay

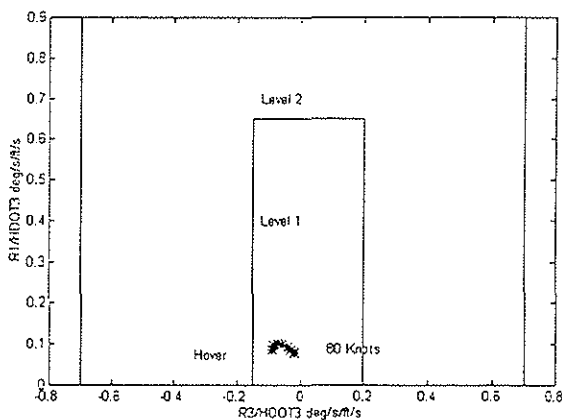


Figure 20. Yaw to collective cross coupling

## Conclusion

A 19th order model of a typical combat rotorcraft flying at 30 knots straight and level flight was analysed using ICA. It was found that at low frequencies the plant is sensitive to becoming non-minimum phase due to the proximity of the  $\Gamma$ 's to the  $(+1,0)$  point, hence there is a potential stability problem. The sensitivity exists as a property of the plant and not as a consequence of the introduction of control. This sensitivity is benign as the pilot can compensate for any low frequency unstable modes

which may arise. A low order diagonal control law was formulated using ICD with special attention given to developing open-loop specifications to meet HQ bandwidth requirements. The design was found to maintain level 1 small signal handling qualities from hover up to 80 knots showing that neoclassical methods can be applied effectively to helicopter flight control. Scope for future work includes assessment of the linear ICD control law using non-linear simulations, to investigate whether the design maintains level 1 response for moderate and large amplitude signals. Flight conditions other than straight and level are being investigated, and the design of response types such as TRC offers further scope as this involves consideration of non-square systems. The effects of such a non-square system on stability robustness will be assessed within the ICAD framework.

## Acknowledgements

The authors wish to thank DRA (Bedford) for supplying them with the HELISTAB and HELISIM packages. Valuable discussions on the subject matter of the paper with Mr. D.J. Diston (British Aerospace Warton), Dr. W.E. Leithead (University of Strathclyde) and Prof. D.J. Murray-Smith (University of Glasgow) are gratefully acknowledged. The opinions expressed in the paper are those of the authors.

## References

1. Handling Qualities Requirements for Military Rotorcraft (ADS-33C), United States Army Aviation Systems Command, St. Louis, MO., Directorate for Engineering, August 1989.
2. M. A. Manness and D. J. Murray-Smith, Aspects of Multivariable Flight Control Law Design for Helicopters Using Eigenstructure Assignment, J. American Helicopter Society, July 1992, 18-32.
3. A. Yue and I. Postlethwaite, Improvement of helicopter handling qualities using  $H^\infty$ -optimisation, IEE Proceedings, Vol. 137, Pt. D, No. 3, May 1990, 115-129
4. J. J. Gribble, Linear Quadratic Gaussian/Loop Transfer Recovery Design for a Helicopter in Low-Speed Flight, J. Guidance, Control and Dynamics, Vol. 16, No. 4, July-August 1993, 754-761.
5. J. O'Reilly and W. E. Leithead, Multivariable control by individual channel design, Int. J. Control, Vol. 54, 1991, 1-46.
6. W. E. Leithead and J. O'Reilly, m-Input m-output feedback control by individual channel design Part 1. Structural issues, Int. J. Control, Vol. 56, 1992, 1347-1397.



7. G. D. Padfield, A theoretical model of helicopter flight mechanics for application to piloted simulation, RAE Technical Report 81048, HMSO, London 1981

8. J. Liceaga-Castro, C. Verde, J. O'Reilly and W. E. Leithead, Helicopter flight control using individual channel design, IEE proc.-Control Theory Appl., Vol. 142, No. 1, January 1995

9. M. B. Tischler, Digital Control of highly Augmented Combat Rotorcraft, NASA-Technical Memorandum 88346, USAAVSCOM Technical Report 87-A-5, May 1987

10. J. Smith, An analysis of helicopter flight mechanics part I - Users guide to the software package HELISTAB, Royal Aircraft Establishment, TM FS(B) 569, October 1984.

**Appendix**

The following state space matrices form the 19th order linear model of a typical combat rotorcraft at 30 knots straight and level flight. The model was produced from HELISTAB [10].

$$A = \begin{bmatrix} A_{\text{rigidbody}} & \vdots & A_{\text{body/rotor}} & \vdots & \\ \dots & \dots & \dots & \vdots & A_{\text{control}} \\ A_{\text{rotor/body}} & \vdots & A_{\text{rotor}} & \vdots & \\ \dots & \dots & \dots & \dots & \dots \\ & 0_A & & \vdots & A_{\text{actuators}} \end{bmatrix}$$

where  $0_A$  is a zero matrix of dimension (4,15) and,

$$A_{\text{rigidbody}} = \begin{bmatrix} 0.0021 & 0.0386 & -3.3486 & -32.1188 & 0.0013 & 0.0366 & 0 & 0 & 0 \\ -0.1632 & -0.5333 & 51.2196 & -2.0858 & -0.0172 & -0.4941 & 1.3028 & 0 & 0 \\ 0.0007 & -0.0011 & -0.1679 & 0 & 0.0001 & 0.0015 & 0 & 0 & 0 \\ 0 & 0 & 0.9992 & 0 & 0 & 0 & 0 & 0.0406 & 0 \\ 0.0120 & -0.0007 & 0.0211 & 0.0847 & -0.0685 & 3.1910 & 32.0923 & -49.7509 & 0 \\ -0.0018 & -0.0027 & 0.0030 & 0 & 0.0002 & 0.0105 & 0 & -0.1203 & 0 \\ 0 & 0 & -0.0026 & 0 & 0 & 1.0000 & 0 & 0.0649 & 0 \\ -0.0112 & -0.0044 & -0.0096 & 0 & 0.0226 & 0.0959 & 0 & -0.6791 & 0 \\ 0 & 0 & -0.0406 & 0 & 0 & 0 & 0 & 1.0013 & 0 \end{bmatrix}$$

$$A_{\text{body/rotor}} = \begin{bmatrix} 0 & 32.0238 & 0 & 0 & 0 & 0 \\ 0 & 0 & 0 & 0 & 0 & 0 \\ 0 & -27.7742 & 0 & 0 & 0 & 0 \\ 0 & 0 & 0 & 0 & 0 & 0 \\ 0 & 0 & -32.0238 & 0 & 0 & 0 \\ 0 & 0.7275 & -160.9087 & 0 & 0 & 0 \\ 0 & 0 & 0 & 0 & 0 & 0 \\ 0 & 1.6150 & -29.0263 & 0 & 0 & 0 \\ 0 & 0 & 0 & 0 & 0 & 0 \end{bmatrix}$$

$$A_{\text{rotor/body}} = \begin{bmatrix} 0 & 0 & 0 & 0 & 0 & 0 & 0 & 0 & 0 \\ 0 & 0 & 0 & 0 & 0 & 0 & 0 & 0 & 0 \\ 0 & 0 & 0 & 0 & 0 & 0 & 0 & 0 & 0 \\ 0.3193 & 1.0481 & -1.7698 & 0 & 0.0355 & 1.0209 & 0 & 0 & 0 \\ -0.1536 & -0.6815 & 32.6434 & 0 & 0.3644 & 72.6358 & 0 & 0 & 0 \\ 0.3988 & 0.1321 & -72.9790 & 0 & 0.5602 & 34.0146 & 0 & 0 & 0 \end{bmatrix}$$

$$A_{\text{rotor}} = \begin{bmatrix} 0 & 0 & 0 & 10 & 0 & 0 \\ 0 & 0 & 0 & 0 & 10 & 0 \\ 0 & 0 & 0 & 0 & 0 & 10 \\ -1514.8 & 0 & 0 & -317 & 0 & -14 \\ -102.1 & -245.3 & -1133.1 & 0 & -317 & -713 \\ 0 & 1127.9 & -245.3 & -2.9 & 713 & -317 \end{bmatrix} \quad A_{\text{actuators}} = \begin{bmatrix} -12.579 & 0 & 0 & 0 \\ 0 & -12.579 & 0 & 0 \\ 0 & 0 & -12.579 & 0 \\ 0 & 0 & 0 & -25.0 \end{bmatrix}$$

$$A_{\text{control}} = \begin{bmatrix} 22.123 & 2.2327 & -0.0002 & 0 \\ -298.31 & -30.107 & 0.0023 & 0 \\ 0.9150 & 0.0923 & 0 & 0 \\ 0 & 0 & 0 & 0 \\ -0.8572 & -0.0864 & 0 & 15.921 \\ 5.6635 & 0.5715 & 0 & -0.9705 \\ 0 & 0 & 0 & 0 \\ 13.788 & 13913 & 0 & -13.071 \\ 0 & 0 & 0 & 0 \\ 0 & 0 & 0 & 0 \\ 0 & 0 & 0 & 0 \\ 0 & 0 & 0 & 0 \\ 740.52 & 62.205 & 0 & 0 \\ -101.28 & -10.212 & 1133.1 & 0 \\ 164.01 & 1134.2 & 0 & 0 \end{bmatrix} \quad B = \begin{bmatrix} \dots & \dots & 0_B & \dots & \dots \\ 12.579 & 0 & & 0 & 0 \\ 0 & 12.579 & & 0 & 0 \\ 0 & 0 & & 12.579 & 0 \\ 0 & 0 & & 0 & 25.0 \end{bmatrix}$$

$$C = \begin{bmatrix} 0.0130 & -0.1994 & 0 & 10.1333 & 0.0081 & 0 & -0.0266 & 0 & 0 & \vdots \\ 0 & 0 & 1146 & 1146 & 0 & 0 & 0 & 0 & 0 & \vdots \\ 0 & 0 & 0 & 0 & 0 & 2.292 & 1146 & 0 & 0 & \vdots \\ 0 & 0 & 0 & 0 & 0 & 0 & 0 & 1146 & 0 & \vdots \end{bmatrix} \begin{matrix} \\ \\ 0_C \\ \end{matrix}$$

where  $0_B$  is a zero matrix of dimension (15,4) and  $0_C$  is a zero matrix of dimension (4,10)

The state vector is,

$$x = [x_{\text{rigidbody}} \quad x_{\text{rotor}} \quad x_{\text{actuator}}]$$

where,

$$x_{\text{rigidbody}} = [u \quad w \quad q \quad \theta \quad v \quad p \quad \phi \quad r \quad \psi]$$

$$x_{\text{rotor}} = [\beta_{\tau 0} \quad \beta_{1c} \quad \beta_{1s} \quad \dot{\beta}_{\tau 0} \quad \dot{\beta}_{1c} \quad \dot{\beta}_{1s}]$$

$$x_{\text{actuator}} = [\theta_{0\text{act}} \quad \theta_{1s\text{act}} \quad \theta_{1c\text{act}} \quad \theta_{0\text{Tact}}]$$